

3.5.4 ICRS Centre

Introduction

The IAU has charged the IERS with the responsibility of monitoring the International Celestial Reference System (ICRS), maintaining its current realization, the International Celestial Reference Frame (ICRF), and maintaining and improving the links with other celestial reference frames. Starting in 2001, these activities are run jointly by the ICRS Centre (US Naval Observatory and Observatoire de Paris) of the IERS and the International VLBI Service for Geodesy and Astrometry (IVS), in coordination with the IAU Working Group on the Reference System. The present report was jointly prepared by the U.S. Naval Observatory and Paris Observatory components of the ICRS Centre. The ICRS Centre web site (<http://hpiers.obspm.fr/icrs-pc>) provides information on the characterization and construction of the ICRF (radio source nomenclature, physical characteristics of radio sources, astrometric behaviour of a set of sources, radio source structure). This information is also available by anonymous ftp ([hpiers.obspm.fr/icrs-pc](ftp://hpiers.obspm.fr/icrs-pc)), and on request to the ICRS Centre (icrspc@hpopa.obspm.fr).

Maintenance and extension of the ICRF: validation of individual VLBI reference frames

The process of maintenance and extension of the ICRF involves the examination and validation of individual reference frames contributed by various international organizations. During 2004, four individual celestial reference frames obtained from VLBI analysis have been validated by comparison with ICRF-Ext. 1.

The reference frames analysed

RSC (AUS) 04 R 01 is the extragalactic celestial frame calculated at Geoscience Australia with VLBI observations acquired in the period April 1980 – May 2004. OCCAM 6.1 software has been used for the solution. The orientation of the celestial frame has been defined through no-net-rotation constraints to the positions of 207 ICRF defining sources. IERS 1996 and MHB2000 have been adopted as the a priori precession and nutation models respectively. Tropospheric gradients have been adjusted in the solution.

RSC (BKGI) 04 R 01 is the extragalactic celestial frame calculated by the Federal Agency for Cartography and Geodesy and the Geodetic Institute of the University of Bonn, in Germany. The software used for the solution is CALC 9.13, SOLVE release 2004.03.18. The celestial reference frame has been oriented by a no-net-rotation constraint to the positions of the 212 defining ICRF sources. The time span of the observations used in the solution is January 1984 – March 2004. The a priori precession and nutation models are both IERS 1996. Tropospheric gradients have been adjusted in the solution.

RSC (CGS) 04 R 01 is the extragalactic radio source catalogue produced by the Space Geodesy Centre in Matera, Italy from ob-

servations in the period April 1980 – October 2003. The software used is CALC 9.12 SOLVE release 2002.10.04, SOLVE revision 2002.10.11. The celestial frame has been oriented by a no-net-rotation imposed to the positions to 141 ICRF defining sources. The a priori precession and nutation models are both IERS 1996. Tropospheric gradients have been adjusted in the solution.

RSC (GAOUA) 03 R 01 is the extragalactic celestial frame from the Main Astronomical Observatory of the National Academy of Sciences of Ukraine, evaluated from observations acquired in the period August 1979 – September 2003. The software used is SteelBreeze-2.0.2. The orientation of the celestial frame has been made by no-net-rotation constraints to 23 ICRF defining sources. The IAU-2000A precession-nutation has been chosen as a priori model for the celestial pole position. Tropospheric gradients have been adjusted in the solution.

Table 1 gives the characteristics of the frames analysed. Four categories of sources appear in the table: *defining*, *candidate* and *other* sources correspond to the classification of ICRF sources (Ma and Feissel, 1997; Ma et al., 1998); *new* are the sources added in ICRF-Ext.1; *additional* represents sources not present in ICRF-Ext.1 but observed in other VLBI programs. The values of the median of the coordinate uncertainties indicate that all frames are of similar quality.

Table 1: Individual VLBI celestial reference frames analysed. n is the number of sources, m is the median of the coordinate uncertainties (unit: mas)

Frame	Total n	Defining n m	Candidate n m	Other n m	New n m	Addit. n m	(°)
RSC (AUS) 04 R 01	571	202 0.13	247 0.18	4 0.25	56 0.20	62 0.36	-81;+84
RSC (BKGI) 04 R 01	668	207 0.07	218 0.07	101 0.03	45 0.12	97 0.23	-81;+84
RSC (CGS) 04 R 01	554	183 0.05	196 0.05	98 0.02	41 0.08	36 0.09	-80;+84
RSC (GAOUA) 03 R 01	1571	211 0.09	244 0.12	101 0.04	51 0.14	964 0.49	-81;+86

Comparison of individual celestial frames to ICRF-Ext.1

The catalogues listed in Table 1 have been compared to ICRF-Ext.1. The algorithm of comparison is the one developed and currently used at the ICRS Centre. The coordinate differences between two frames are modelled by a global rotation of the axes, represented by the angles A_1, A_2, A_3 , and by deformations represented by three parameters: D_α is a slope in right ascension as a function of the declination, D_δ is a slope in declination as a function of the declination, B_δ is a bias between the principal plane of the frame and that of ICRF-Ext.1.

$$\begin{aligned}
 A_1 \operatorname{tg} \delta \cos \alpha &+ A_2 \operatorname{tg} \delta \sin \alpha &- A_3 &+ D_\alpha (\delta - \delta_0) &= \Delta \alpha \\
 - A_1 \sin \alpha &+ A_2 \cos \alpha &&+ D_\delta (\delta - \delta_0) + B_\delta &= \Delta \delta
 \end{aligned}$$

Under the hypothesis that ICRF-Ext.1 is free from deformations, the systematic effects detected in the comparisons should be interpreted as deformations in the individual frames.

Defining sources common to each individual frame and ICRF-Ext.1 have been used for the comparisons. The six parameters have been evaluated by a weighted least squares fit; the equations have been weighted using the inverse of the variance of the coordinate differences.

In the individual frames, formal uncertainties in radio source positions smaller than 0.01 mas were set to this value for the assignment of weights. The fitted parameters allow the transformation of coordinates in the individual frames into ICRS. Radio sources with residuals higher than 2.5 the rms residual of the fit are considered as outliers, and consequently deweighted.

Results The results of the comparisons are shown in Tables 2 to 4. Table 2 gives the global orientation between the axes of the individual frames analysed and those of the ICRS. Table 3 gives the values of the deformation parameters representing systematic effects in the individual frames. Table 4 gives the values of the rms and the weighted mean residuals.

Table 2: Relative orientation between individual frames and ICRF-Ext.1. N is the number of the common defining sources in each individual frame used for the comparison. Unit: μas .

Frame	N	A_1	A_2	A_3
RSC (AUS) 04 R 01	202	-24.02 ± 19.39	$+49.64 \pm 19.17$	-3.67 ± 24.91
RSC (BKGI) 04 R 01 ⁽¹⁾	207	-3.61 ± 17.86	-19.19 ± 17.75	-32.28 ± 22.95
RSC (CGS) 04 R 01 ⁽²⁾	183	$+16.46 \pm 22.49$	$+38.52 \pm 22.35$	$+7.44 \pm 30.67$
RSC (GAOJA) 03 R 01	211	$+13.70 \pm 18.63$	$+39.16 \pm 18.52$	-21.72 ± 23.87

(1): one source has been deweighted

(2): four sources have been deweighted

Table 3: Slopes and biases evaluated in the comparisons between VLBI individual reference frames and ICRF-Ext.1. D_α , D_δ are the slopes in right ascension and declination respectively, B_δ is the bias in declination; units are $\mu\text{as}/\text{deg}$ for the slopes, μas for the bias.

Frame	N	D_α	D_δ	B_δ
RSC (AUS) 04 R 01	202	-1.79 ± 0.78	$+0.10 \pm 0.42$	$+15.32 \pm 21.26$
RSC (BKGI) 04 R 01 ⁽¹⁾	207	-0.95 ± 0.73	-0.81 ± 0.38	$+19.88 \pm 18.65$
RSC (CGS) 04 R 01 ⁽²⁾	183	-0.73 ± 1.01	-0.85 ± 0.56	$+34.96 \pm 27.08$
RSC (GAOJA) 03 R 01	211	-0.84 ± 0.76	-0.43 ± 0.39	-8.47 ± 19.40

(1): one source has been deweighted

(2): four sources have been deweighted

Table 4: Weighted mean residuals r_α and r_δ , and rms residual after fitting the global rotations and the deformation parameters between individual frames and ICRF; unit is μas .

Frame	r_α	r_δ	rms
RSC (AUS) 04 R 01	-2.18	-3.68	257.73
RSC (BKGI) 04 R 01	-6.73	+0.89	239.13
RSC (CGS) 04 R 01	+0.43	+2.58	277.89
RSC (GAOUA) 03 R 01	-9.47	-2.24	252.37

The values of the angles A_1, A_2, A_3 in Table 2 show that the individual reference frames realize the axes of the ICRF better than $50 \mu\text{as}$, and their uncertainties indicate that, after rotation, the inconsistency between the directions of the axes is at most $30 \mu\text{as}$.

There is no evidence of deformations in the coordinates depending on the declination (see values of D_α, D_δ in Table 3); the principal planes of some of the individual frames are biased with respect to that of ICRS, this being the case of RSC (CGS) 04 R 01 ($+34.96 \mu\text{as}$), and with smaller amplitude, of RSC (BKGI) 04 R 01 and RSC (AUS) 04 R 01. The values of r_α and r_δ in Table 4 indicate that the model represents well the inconsistencies between the orientations of frames at a level of $10 \mu\text{as}$ or better.

E. Felicitas Arias, Anne-Marie Gontier, C. Barache

Investigation of future realizations of the ICRS

Involvement by ICRS Centre personnel in the celestial reference frame VLBI program continued in 2004, increasing the number of observations of ICRF quasars in the southern celestial hemisphere and continuing an extensive observing program in the northern hemisphere. This observing program will eventually result in a future extension and potentially a new realization of the ICRS. In the Southern Hemisphere, the USNO and the Australia Telescope National Facility (ATNF) are collaborating in a continuing VLBI research program in Southern Hemisphere source imaging and astrometry using USNO, ATNF and ATNF-accessible facilities. These observations are aimed specifically toward improvement of the ICRF in the Southern Hemisphere by a) increasing the reference source density with additional S/X-band bandwidth-synthesis astrometric VLBI observations, and b) VLBI imaging at 8.4 GHz of ICRF sources south of $\delta = -20^\circ$. In the Northern Hemisphere a major source of VLBI data continues to be the series of RDV experiments, which consist of observations of International Celestial Reference Frame (ICRF) sources at radio frequencies of 2.3 GHz and 8.4 GHz using the Very Long Baseline Array (VLBA), together with up to 10 geodetic antennas. These VLBA RDV observations constitute a joint

program between the U.S. Naval Observatory (USNO), Goddard Space Flight Center (GSFC) and the National Radio Astronomy Observatory (NRAO) for maintenance of the celestial and terrestrial reference frames. During calendar year 2004, six VLBA RDV experiments were observed. In addition VLBA observations to extend the ICRF to K-band (24 GHz) and Q-band (43 GHz) continued in 2004. These observations are part of a joint program between the National Aeronautics and Space Administration, the USNO, the National Radio Astronomy Observatory (NRAO) and Bordeaux Observatory.

In the coming decades, there will be significant advances in the area of space-based optical astrometry. Proposed and scheduled missions such as the National Aeronautics and Space Administration's (NASA) *Space Interferometry Mission* (SIM) and the European Space Agency's (ESA) *Gaia* mission will achieve positional accuracies well beyond that presently obtained by any ground-based radio interferometric measurements. In 2004, ICRS Centre personnel continued their participation in the NASA SIM mission, through direct involvement in one of the SIM key science projects: *Astrophysics of Reference Frame Tie Objects*. In addition, during 2004 ICRS Centre personnel were funded by NASA to lead and execute a concept study for the *Origins Billions Star Survey* (OBSS) mission, a unique astrometric and astrophysical Galactic Exploration mission that will leave as a legacy the measurement of over two billion stellar positions, parallaxes, and proper motions, along with a scientifically rich database of extrasolar planet detections, binarity determinations, stellar photometry and variability, and low resolution spectrometry. Conclusion of the 8 month OBSS concept study was expected to continue into early 2005.

*Ralph A. Gaume, Alan L. Fey, Norbert Zacharias,
David A. Boboltz*

Monitor source structure to assess astrometric quality

VLBA RDV Imaging

Observations of International Celestial Reference Frame (ICRF) sources at radio frequencies of 2.3 GHz and 8.4 GHz using the Very Long Baseline Array (VLBA), together with up to 10 geodetic antennas, continued in 2004. These VLBA RDV observations constitute a joint program between the U.S. Naval Observatory (USNO), Goddard Space Flight Center (GSFC) and the National Radio Astronomy Observatory (NRAO) for maintenance of the celestial and terrestrial reference frames. During the calendar year 2004, six VLBA RDV experiments were observed.

VLBA experiment RDV45 (2004JUL14) was calibrated and imaged, adding 160 (80 S-band; 80 X-band) images to the Radio Reference Frame Image Database including images of 11 sources (0316+413, 0426+273, 0602+673, 0620+389, 0656+082, 1030+074, 1226+023,

1240+381, 1417+385, 1738+499, 2235+731) not previously imaged. Unlike previous RDV experiments, the data from the geodetic antennas were flagged before processing leaving only the data obtained by the VLBA. This was done in an attempt to reduce the amount of time required to image these experiments by decreasing the amount of data actually used for imaging. The resultant images are essentially VLBA only, but in some instances have lower resolution due to the sub-netting of the array during the RDV observations. A comparison of the angular resolution of the images with previous experiments showed that on average the resolution of the RDV45 images is about a factor of 1.6 times worse than for a full RDV experiment and about a factor of 1.1 times worse than for a VLBA only experiment (i.e. a VLBA experiment with no sub-netting). The consensus opinion reached was that the resulting lower resolution images would hinder structure analysis. Future RDV experiments will be processed with all available data.

VLBA High Frequency Imaging

VLBA observations to extend the ICRF to K-band (24 GHz) and Q-band (43 GHz) continued in 2004. These observations are part of a joint program between the National Aeronautics and Space Administration, the USNO, the National Radio Astronomy Observatory (NRAO) and Bordeaux Observatory. During the calendar year 2004, two VLBA high frequency experiments (BL115B and BL115C) were calibrated, imaged and added to the Radio Reference Frame Image Database.

ICRF Maintenance in the Southern Hemisphere

The USNO and the Australia Telescope National Facility (ATNF) are collaborating in a continuing VLBI research program in Southern Hemisphere source imaging and astrometry using USNO, ATNF and ATNF-accessible facilities. These observations are aimed specifically toward improvement of the ICRF in the Southern Hemisphere by a) increasing the reference source density with additional S/X-band bandwidth-synthesis astrometric VLBI observations, and b) VLBI imaging at 8.4 GHz of ICRF sources south of $\delta = -20^\circ$.

VLBI images for a total of 69 Southern Hemisphere ICRF sources at a frequency of 8.4 GHz using the Australian Long Baseline Array were published by Ojha et al. (2004) and added to the Radio Reference Frame Image Database. The images were used to calculate a core fraction, i.e., the ratio of core flux density to total flux density, for all observed sources. The resulting distribution, with a mean value of 0.83, suggests that most sources are relatively compact. However, just over half the observed sources show significant extended emission in the form of multiple compact components. Images for an additional 60 sources have been made and are being prepared for publication.

The Radio Reference Frame Image Database

The Radio Reference Frame Image Database (RRFID) is a web accessible database of radio frequency images of ICRF sources. The RRFID currently contains 3285 VLBA images of 463 sources at radio frequencies of 2.3 GHz and 8.4 GHz. Additionally, the RRFID contains 783 images of 231 sources at frequencies of 24 GHz and 43 GHz. The RRFID can be accessed from the Analysis Centre web page or directly at <http://www.usno.navy.mil/RRFID/>.

A recent addition to the RRFID are Australian Long Baseline Array (LBA) images of 69 southern hemisphere ICRF sources at a radio frequency of 8.4 GHz.

Quantifying Source Structure

The images from the RRFID can be used to classify the sources in terms of their suitability for astrometric use based on their spatial compactness. The CLEAN component model from an image is used to calculate the visibility amplitude, $V(r, \phi)$, in the u, v plane at 24 equally spaced baseline position angles, ϕ , spanning 180° and at 300 equally spaced u, v radii, r , (i.e. baseline lengths) ranging from zero to one Earth diameter.

The visibility amplitude is then averaged over baseline position angle at each u, v radii and then normalized by the zero spacing amplitude. The result is an estimate, $V(r)/V(0)$, of the “average” visibility amplitude change as a function of baseline length, r .

The next step is to calculate the standard deviation, $\sigma_v(r)$, over all baseline position angles, ϕ , for each u, v radii and then divide $\sigma_v(r)$ by $V(r)$ at each u, v radii. The result is a normalized estimate, $\sigma_v(r)/V(r)$, of the azimuthal asymmetry of the source, i.e. if the source is mostly circular, then $\sigma_v(r)/V(r)$ at all baseline lengths, r , will be small. If the source is highly elliptical, then $\sigma_v(r)/V(r)$ will become increasingly larger with increasing baseline length.

Finally, we calculate an estimate of the radio astrometric quality of the observed sources. For each observed source, a score is tabulated based on the following (higher scores are better):

- **compactness**: range [0 – 20], i.e., $20 \times [V(r_1)/V(0)]$ where r_1 is the u, v radius at which $V(r)/V(0)$ reaches a minimum ($r_1 \leq r_x$)
- **asymmetry**: range [0 – 40], i.e., $40 \times [1 - \sigma_v(r_2)/V(r_2)]$ where r_2 is the u, v radius at which $\sigma_v(r)/V(r)$ reaches a maximum ($r_2 \leq r_x$)
- **baseline**: range [0 – 40], i.e., $40 \times [r_x/r_{\max}]$ where r_x is the u, v radius at which the normalized “average” visibility and its normalized variation first intersect and r_{\max} is the maximum u, v radius

The last step is to sum the score for each source. The result is an estimate of radio astrometric quality, Q , and ranges from zero (for the worst astrometric sources) to one hundred (for the best astrometric sources).

Examples of $V(r)/V(0)$ and $\sigma_v(r)/V(r)$ calculated at an observing frequency of 8.4 GHz for several simple source models are shown

in Figure 1. An example for the source 0138–097 at epoch 2004 Feb 15 is shown in Figure 2.

Initially applied to the high frequency (K/Q-band) data, the method has not yet been applied to the study of ICRF sources at the standard S/X frequencies.

Alan L. Fey, David A. Boboltz

Impact of the stability of the VLBI celestial reference frame on the determination of the sidereal orientation of the Earth

Following studies of the stability of radio source coordinates, Feissel-Vernier et al. (2005) studied the influence of the effective celestial reference frame on the derived precession, nutation and universal time. They showed that taking the most stable sources as the basis for defining the celestial reference frame orientation and treating the most unstable sources as arc sources improves the reference frame internal consistency at the level of 30% in the variance of source declinations. As a result, the determination of precession

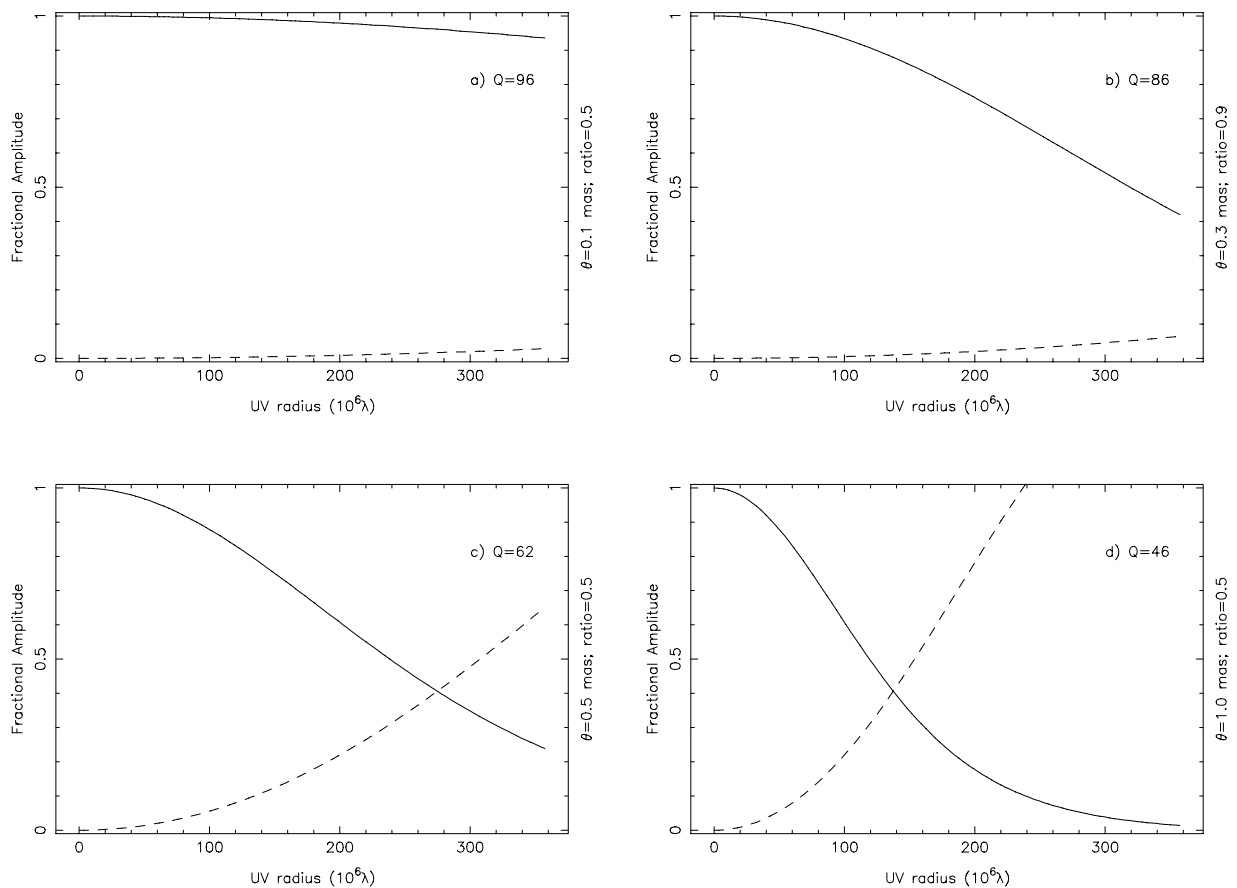


Fig. 1: Normalized “average” visibility, $V(r)/V(0)$ (solid line), and its normalized variation, $\sigma_v(r)/V(r)$ (dashed line), calculated at an observing frequency of 8.4 GHz. Source models are single Gaussian components with a) angular size, $\theta = 0.1$ mas, axial ratio, $R = 0.5$; b) $\theta = 0.3$ mas, $R = 0.9$; c) $\theta = 0.5$ mas, $R = 0.5$; d) $\theta = 1.0$ mas, $R = 0.5$. Q is an estimate of the radio astrometric quality which ranges from zero (for the worst astrometric sources) to one hundred (for the best astrometric sources).

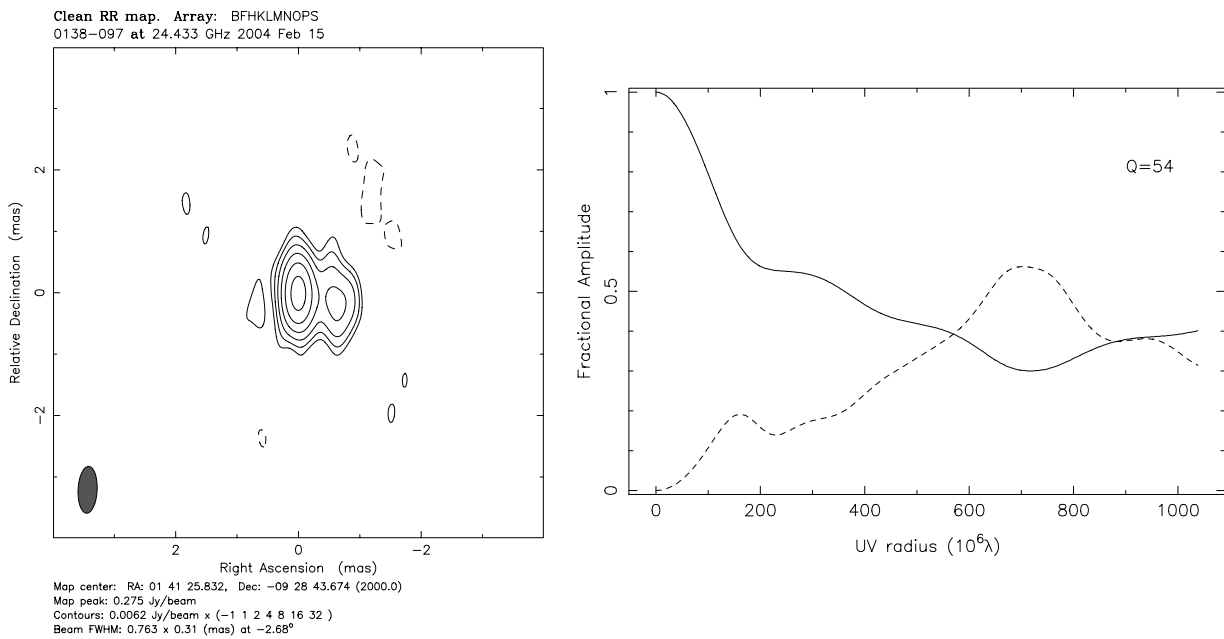


Fig. 2: Contour plot of the radio emission at K-band (24 GHz) from the source 0138-097 at epoch 2004Feb15; Right panel: Normalized “average” visibility, $V(r)/V(0)$, (solid line) and its normalized variation, $\sigma_v(r)/V(r)$, (dashed line) for the same source.

and nutation components is affected at various levels, depending on their frequency. In the seasonal and FCN frequency band, the effect is small in the 1980s and negligible in the 1990s. In the two-to three-year frequency band, it was shown that, even when considering the most stable sources, source instabilities may mimic transient oscillations with an amplitude up to 20 μs . For what concerns the principal term of nutation, the actual departure of VLBI results with the IAU2000 model may reach 50 μs in $\Delta\epsilon$ and 320 μs in $\Delta\psi$. The latter discrepancy is larger than the 80 μs discrepancy mentioned by the authors of the IAU2000 Nutation model. The influence on the determination of the precession correction and the secular obliquity rate is lower than 10 μs . The precession correction departure from the IAU2000 model excluding the unstable sources is quite larger than that based on all sources. This discrepancy is not modified by the source instability effect. Finally, the departures from the IAU2000 values stay around 50 $\mu\text{s}/\text{year}$ in precession and 30 $\mu\text{s}/\text{year}$ in obliquity rate. The contribution of the instability of the right ascensions to the instability of the VLBI-derived UT1 was found to stay under one microsecond at J2000.0 and 0.5 $\mu\text{s}/\text{year}$, for both the conventional and proposed source selections. A possible common effect in right ascensions, with a period of six years and an amplitude of 15 μs , is suggested by the analysis of the use of the proposed source selection. Because of converging evidences about the improvement of the internal con-

sistency of VLBI-derived celestial reference frames brought by the consideration of source stability, we suggest that future investigations of precession and nutation and sidereal time of the global Earth take full account of this new aspect of the VLBI data.

Martine Feissel-Vernier

Maintenance of the link to the Hipparcos catalog

During the reporting period (2004) progress has been achieved at USNO in 4 areas related to the maintenance of the Hipparcos link: UCAC project (current epoch observing and early epoch data), the extragalactic link, and URAT.

All-sky coverage was reached in May 2004 with the USNO CCD Astrograph. The last deep CCD fields were taken in December 2004 with the KPNO 0.9-meter telescope and parallel observing with the astrograph. This concludes the observational part of the UCAC project. By end of 2004 about 50% of the raw pixel data were loaded to RAID disk space in preparation for a final reduction of the UCAC data. UCAC3, the final catalog, will be released by mid 2006 at earliest. Measuring of Hamburg Zone astrograph and USNO Black Birch plates continued on StarScan (USNO plate measuring machine). These data will provide the first epoch for several million of stars to 14th magnitude, as part of UCAC3.

Deep CCD images of ICRF optical counterparts were obtained in a total of 25 observing runs at KPNO and CTIO between December 1997 and December 2004. In October 2004 first results were presented at the Lowell, Flagstaff, AZ astrometry meeting. For the first time the dedicated astrograph wide-field observations taken in parallel, providing the secondary reference stars for the link. A large fraction of the 16 sources observed in the first 2 nights of the June 2001 KPNO 2.1m run show (optical-radio) position offset errors in the 10 to 20 mas range, better than anything else achieved to date.

Monitoring of a sample of 12 ICRF optical counterparts continued at the Naval Observatory Flagstaff Station (NOFS) 1.55-meter telescope. This effort is part of the SIM preparatory science for the celestial reference frame key project (K. Johnston, PI).

Optical design studies matured during 2004 for the USNO Robotic Astrometric Telescope (URAT). This will be a dedicated 0.85-meter aperture, 3-degree wide-field telescope for an all-sky survey to 20th magnitude with a goal of 5 to 10 mas positional errors on the HCRF for the 14th to 18th magnitude range. This telescope will be capable of directly linking to ICRF optical counterparts and to bright Hipparcos stars with special observing procedures. A detector development (large monolithic chip) was funded through a U.S. government Small Business Innovation in Research (SBIR) grant. The goal for first light is 2007.

Norbert Zacharias, Alan L. Fey, David A. Boboltz

Linking the ICRF to frames at various wavelengths

The number of recorded quasars at optical wavelengths has noticeably increased in the recent years, reaching the number of 48921 objects in a compilation of various catalogues (Véron-Cetty and Véron, 2003). Therefore, following the cross-identification between the above catalogue and the ICRF (see IERS Annual Report, 2003) showing that roughly 67% of the quasars belonged to the two catalogues, some photometric and astrometric properties of the cross-identified objects could be obtained. They show in particular that the quasars of the ICRF have been chosen so that their flux at 6cm is ranged for a large proportion between 0.5 Jy and 1.5 Jy, whereas the peak for the quasars of the Véron-Cetty and Véron compiled catalogue (quoted in the following as VCV catalogue) is roughly 5.0 Jy. Concerning the V-magnitudes of the objects, the histogram shows clearly a peak in the number of ICRF quasars between $V = 18.0$ and $V = 18.5$ whereas the majority of objects of the VCV catalogue is ranged between $V = 19.0$ and $V = 20.5$. Other histograms concerning the red-shifts show that ICRF contains proportionally much more objects with rather low red-shifts (more than 50% of quasars with $z < 1.5$) in comparison with VCV objects, for which the majority of quasars corresponds to the zone $1.0 < z < 2.5$.

Jean Souchay

Maintenance of the link to the solar system dynamical reference frame using Lunar Laser Ranging (LLR) analyses

The dynamical reference frame is materialized by the dynamical ecliptic and equinox (epoch J2000.0) related to the orbit of the Moon through the ephemerides of the lunar solution ELP (Chapront-Touzé M. and Chapront J.). The analysis of the LLR observations enables the orientation of dynamical ecliptic and equinox of J2000.0 with respect to ICRS.

The orientation of the dynamical ecliptic reference frame can be also obtained with respect to the reference frame linked to the mean Celestial Ephemeris Pole (CEP), noted here MCEP.

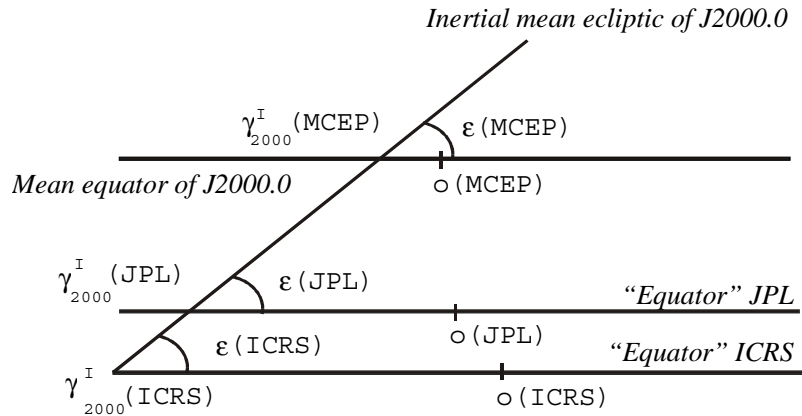
Using the lunar ephemerides produced by the Jet Propulsion Laboratory (JPL) numerical integrations considered as 'observational models' instead of the LLR data, the dynamical reference frame can also be linked to the reference frames defined by these JPL numerical integrations (as DE403 or DE405).

The basic definitions are (see the figure) :

- (R) Equatorial reference frame (ICRS, MCEP, JPL),
- γ_{2000}^l (R) Ascending node of the 'inertial' mean ecliptic J2000.0 on the equator of (R),
- o (R) Origin of right ascensions on the equator of (R),
- ε (R) Inclination of the inertial mean ecliptic to the equator of (R),
- φ (R) Arc between o (R) and γ_{2000}^l (R) on the equator of (R),
- ψ (R) Arc between γ_{2000}^l (ICRS) and γ_{2000}^l (R) on the mean ecliptic of J2000.0.

3.5.4 ICRS Centre

Remark : $\gamma_1^{(MCEP)}$ is named the ‘inertial’ dynamical mean equinox of J2000.0; the separation from $\gamma_1^{(MCEP)}$ to the ‘rotational’ dynamical mean equinox of J2000 $\gamma_R^{(MCEP)}$ is 93.66 mas.



The evaluation of the angles $\epsilon(R)$, $\phi(R)$ and $\psi(R)$ are involved in the transformation of the rectangular coordinates of the LLR stations in the terrestrial reference frame to the celestial equatorial coordinates at the epoch J2000.0 taking into account the polar motion, the Earth rotation and the orientation of the celestial pole (precession-nutation matrix).

This transformation has been realized according to the lunar solution which results from weighted fits of the semi-analytical theory ELP of the orbital motion of the Moon to the LLR observations provided between 1970 and 2004 by the LLR stations: 9361 from Grasse (Observatoire de la Côte d’Azur, France), 6920 from Fort-Davis (McDonald Observatory, Texas) and 482 from Manui (Haleakala Observatory, Hawaii).

The position of the inertial dynamical ecliptic of J2000 with respect to the ICRS is defined by the angles $\epsilon^{(ICRS)}$ and $\phi^{(ICRS)} = \circ^{(ICRS)}\gamma_1^{(ICRS)}$. In this case, the precession-nutation matrix is computed with the IERS conventions using the daily corrections of the nutation in longitude and obliquity provided by IERS (Earth Orientation Centre series C04).

The position of the inertial dynamical ecliptic of J2000 with respect to the MCEP is defined by the angles $\epsilon^{(MCEP)}$, $\phi^{(MCEP)} = \circ^{(MCEP)}\gamma_1^{(MCEP)}$ and $\psi^{(MCEP)} = \gamma_1^{(ICRS)}\gamma_1^{(MCEP)}$. In this case, the precession-nutation matrix is provided by analytical solutions.

The comparison between the ephemerides of the lunar solution ELP and the JPL ephemerides DE403 and DE405 enables the evaluation of the angles $e^{(JPL)}$, $j^{(JPL)} = \circ^{(JPL)}g_1^{(JPL)}$ and $y^{(JPL)} = g_1^{(ICRS)}g_1^{(JPL)}$.

The values of these angles are given in the following table.

Frame (R)	$\varepsilon - 23^{\circ}26'21''$	$\varphi (")$	$\psi (")$
ICRS	0.41128 ± 0.00009	-0.05419 ± 0.00009	
MCEP	0.40585 ± 0.00009	-0.01410 ± 0.00011	0.0440 ± 0.0002
DE403	0.40928 ± 0.00001	-0.05294 ± 0.00001	0.0041 ± 0.0004
DE405	0.40960 ± 0.00001	-0.05028 ± 0.00001	0.0055 ± 0.0003

The uncertainties mentioned here represent formal uncertainties resulting from the least square fitting. Realistic uncertainties can be estimated between five and ten times these values.

The LLR analysis give also a determination of the correction Δp to IAU 1976 precession constant. The value obtained with the LLR data collected from 1970 to 2004 is :

$$\Delta p = -3.07 \pm 0.04 \text{ mas/yr}$$

Orbital parameters of the Moon and of the Earth-Moon barycenter have also been fit after comparison between ELP model and LLR data, in particular the tidal component of the secular acceleration of the lunar longitude Γ which is related to a decrease in Earth's rotation rate and an increase of the length of the day. The last determination is:

$$\Gamma = -25.858 \pm 0.003 \text{ "/cy}^2$$

Jean Chapront, Gérard Francou, Sébastien Bouquillon

Link to the solar system dynamical reference frame through pulsar analysis

Pulsar timing observations at the Nançay's radiotelescope have been carried out intensively during the whole year 2004, and specific studies have been devoted to the link between a rigid system related to the pulsars and the dynamical reference frame materialized by the ecliptic. As a first step we have studied the influence of the ephemerides of the solar system used in the reductions (to determine the position of the Earth on its orbit), on the positions of the pulsars themselves. A preliminary test (Souhay and Cognard, 2005) was done starting from a set of 5 pulsars (PSR1821-24, PSR1937+21, PSR1855+09, PSR0613-02 and PSR1643-12). The choice was done between three different kinds of ephemerides of the JPL (Jet Propulsion Laboratory), that is to say DE200, DE405 and DE407. We showed that although the equatorial coordinates of the pulsars were highly dependent on the ephemerides used, the uncertainties on the angular arcs between the pulsars were far smaller, by one or two orders, reaching for some of them the sub-milliarcsecond level. We schedule to keep on this kind of analysis with a larger set of 25 pulsars observed on a regularly basis. Our hope is to construct an astrometric pulsar catalogue in the near future, based on the arcs inter-pulsars and nearly insensitive to the ephemerides used.

Ismael Cognard, Jean Souhay

3.5.4 ICRS Centre

Staff	Gaume	Ralph	Director	(USNO)
	Souchay	Jean	Co-director	(OP)
	Arias	Felicitas	Assoc. Astronomer	(BIPM / OP)
	Boboltz	David	Astronomer	(USNO)
	Bouquillon	Sébastien	Post-doc	(OP)
	Chapront	Jean	Astronomer	(OP)
	Chapront-Touzé	Michelle	Astronomer	(OP)
	Cognard	Ismaël	Astronomer	(LPCE Univ. Orléans)
	Feissel-Vernier	Martine	Astronomer	(OP)
	Fey	Alan	Astronomer	(USNO)
	Francou	Gérard	Astronomer	(OP)
	Gontier	Anne-Marie	Astronomer	(OP)
	Zacharias	Norbert	Astronomer	(USNO)

- References**
- Chapront, J., Chapront-Touzé, M., 1997: Lunar motion, theory and observations, *Celest. Mech.* **66**, 31
- Feissel-Vernier, M., Ma, C., Gontier, A.-M., Barache, C., 2005: *Astron. Astrophys.*, **438**, 1141
- Ma, C., Feissel, M. (eds.), 1997: IERS Technical Note No. 23, Observatoire de Paris.
- Ma, C., Arias, E.F., Eubanks, T.M., Fey, A., Gontier, A.-M., Jacobs, C.S., Sovers, O.J., Archinal, B.A., Charlot, P., 1998: *Astron. J.*, **116**, 516
- Ojha, R. et al., 2004: *Astron. J.*, **127**, 3609
- Souchay, J., Cognard, I., 2005: IERS Technical Note No. 34, in prep.
- Véron-Cetty, M.P., Véron, P., 2003: *Astron. Astrophys.* **412**, 399